An Investigation of the Onsets of the 1999 and 2000 Monsoons in Central Nepal

TIMOTHY J. LANG AND ANA P. BARROS

Division of Engineering and Applied Sciences, Harvard University, Cambridge, Massachusetts

(Manuscript received 1 May 2001, in final form 14 November 2001)

ABSTRACT

The Marsyandi River basin in the central Nepalese Himalayas is a topographically complex region, with strong spatial gradients of precipitation over various timescales. A meteorological network consisting of 20 stations was installed at a variety of elevations (528–4435 m) in this region, and measurements of rainfall were made during the 1999 and 2000 summer monsoons. The onsets of the 1999 and 2000 monsoons in central Nepal were examined at different spatial scales by using a combination of rain gauge, *Meteosat-5*, Tropical Rainfall Measuring Mission (TRMM), ECMWF analysis, and Indian radiosonde data. At the network, the onsets manifested themselves as multiday rain events, which included a mixture of stratiform and convective precipitation. Moist and unstable upslope flow was associated with the occurrence of heavy rainfall. During each onset, 2-day rainfall reached as high as 462 mm, corresponding to 10%–20% of the monsoon rainfall. Differences among rain gauges were up to a factor of 8, reflecting the role of small-scale terrain features in modulating rainfall amounts. At the larger scale, the onsets were associated with monsoon depressions from the Bay of Bengal that moved close enough to the Himalayas to cause the observed upslope flow from the winds on their eastern flank. During the 1999 onset, convection in this eastern flank collided with the mountains in the vicinity of the network. In 2000 no major collision occurred, and 33%–50% less rain than 1999 fell. Analysis of observations for a 5-yr period (1997–2001) suggests that the interannual variability of the monsoon onset along the Himalayan range is linked to the trajectories and strength of these depressions.

1. Introduction

The Himalayas, in particular the south-facing slopes, have not been studied extensively from a meteorological perspective. There is little that is understood about basic interactions between weather systems and the complex topographical features in the region, as well as how these interactions may compare to those in other parts of the world. Because precipitation plays a critical role in modulating the space–time distribution of latent heating, a better understanding of the spatial and temporal variability of rainfall in the Himalayas should be extremely important to improve our understanding of Asian monsoon (and climate) dynamics (e.g., Luo and Yanai 1984).

A major cause of the lack of studies is the remoteness of the region, and the resultant lack of meteorological data. For instance, within the mountainous nation of Nepal, in the central Himalayan region, there are no weather radars or radiosonde stations. In addition, most rain gauges in the Nepalese mountains actually are placed at the bottom of river valleys, leaving gaps in understanding and quantifying precipitation along the ridges.

In one of the few studies done in Nepal, Shrestha (2000) estimated that Nepal as a whole receives approximately 80% of its annual precipitation during the summer monsoon. Using 32 yr of records (1957–1988) from 60 rain gauges distributed along the populated valleys and in the Terai plains, monsoon rainfall totals under 200 cm were estimated for the middle and high Himalaya regions. Shrestha (2000) found a significant relationship between Nepalese rainfall and the Southern Oscillation index (SOI), as well as evidence for the modulation of rainfall totals by terrain. However, being a climatological study, Shrestha (2000) did not go into the details of how individual weather systems interact with the local topography.

A few other studies have examined orographic effects on precipitation in the Himalayas, but generally on timescales longer than that of individual weather systems (Singh et al. 1995; Seko 1987; Dhar and Rakhecha 1981). These studies were based mostly on gauges placed in river valleys, and gave conflicting results on how rainfall varied with elevation. It is unclear whether any of these relationships would hold along ridges, between valleys and ridges, at timescales of individual weather events, or in different regions of the Nepalese Himalayas.

Corresponding author address: Dr. Ana P. Barros, Division of Engineering and Applied Sciences, Harvard University, Pierce Hall 118, 29 Oxford Street, Cambridge, MA 02138.
E-mail: barros@deas.harvard.edu

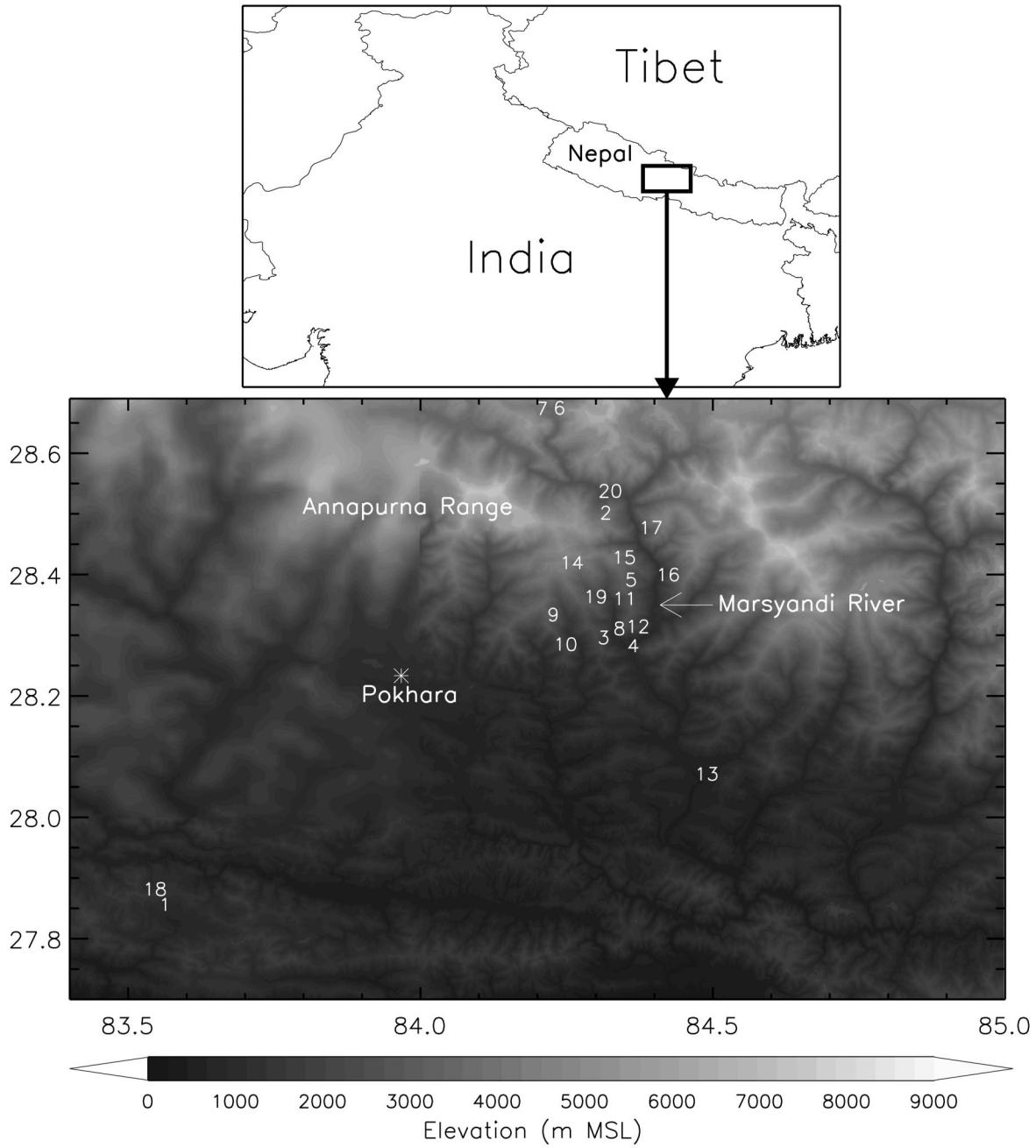

FIG. 1. Topographic map of the Marsyandi River basin, showing locations of the meteorological stations in the network. Station numbers correspond to those in Table 1. Also shown are various landmarks in the region, including the city of Pokhara. The large-scale map shows the location of the network relative to southern Asia.

In order to study orographic effects on precipitation within the south-facing slopes of the Himalayas, a meteorological network was installed within the Marsyandi River basin in central Nepal during the spring of 1999. The Marsyandi River, a tributary to the hydrologically important Ganges River, flows out of the eastern side of the Annapurna Range. The core of the meteorological network (Fig. 1, Table 1), originally described in Barros et al. (2000), consists of rain gauges placed at a variety of elevations, from 528 m to 4435 m MSL. Gauges have been placed along three ridges that jut southward from the eastern Annapurnas. In addition, there are rain gauges in the river valley south and east of these ridges, as well as in the dry region to the north of the Annapurnas. Thus, the network provides an excellent platform with which to study topographical effects on the spatial and

temporal variability of precipitation, as well as to understand monsoon rainfall in the Himalayas.

Barros et al. (2000) reported on the first set of measurements from the new Marsyandi meteorological network, for the 1999 summer monsoon. The data showed that significant rain, ranging from 130 to nearly 400 cm, fell in this area during the monsoon. In particular, Barros et al. (2000) showed that rainfall amounts greater than 300 cm fell at high elevations (≥2000 m MSL). The 1999 monsoon rainfall demonstrated substantial variability, on the seasonal scale, between stations separated by less than a few km. Given the steep altitudinal gradients in this region—elevation differences of several thousand meters over 10 km or less are common—orographic effects on rainfall obviously are very important.

Further analysis of data from the Marsyandi network, for both 1999 and 2000, revealed that the onsets of the monsoons were very important for the seasonal rainfall in central Nepal. Many stations received more than 10%–20% of their seasonal rainfall during the 2–3 days associated with the monsoon onsets, and a few stations received more than a third. In addition, onset rainfall showed large variability, up to a factor of 8, between stations—similar to the previously documented variability at the seasonal timescale. These data have strong implications for understanding the hydrology and geomorphology of the region, especially with regard to erosion and hill slope stability as landslides are one of the most devastating hazards of the monsoon.

In order to understand why the onset rainfall was so large as well as so variable, the 1999 and 2000 monsoon onsets were analyzed, using a variety of meteorological data at multiple spatial scales. In addition, these data were used to investigate the relationships between the onsets in central Nepal and the evolution of the broader Asian monsoon system.

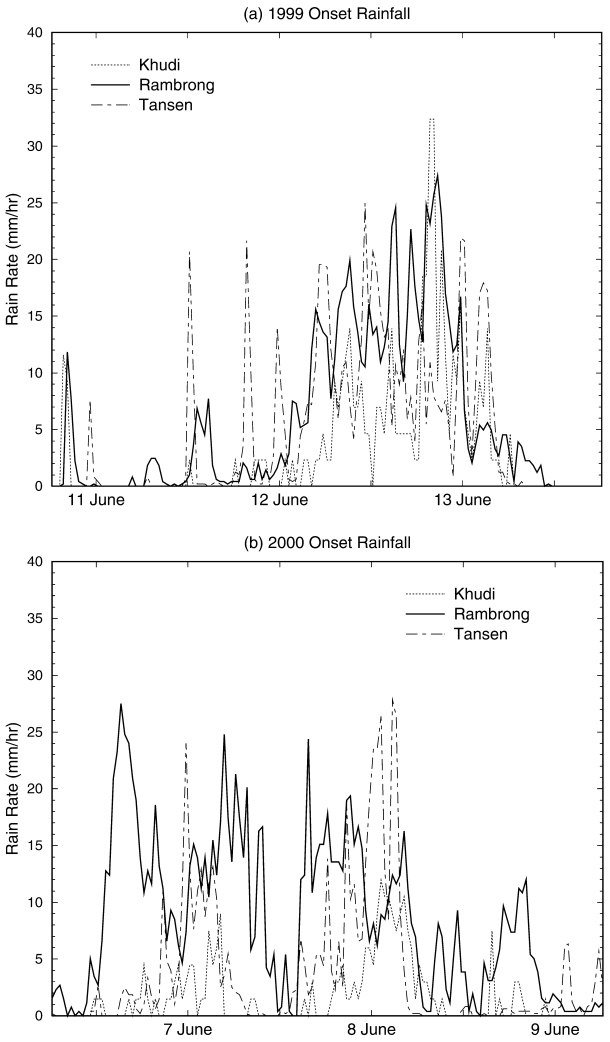

FIG. 2. (a) Time series of rain accumulations at various network stations during the 1999 onset. (b) Same as in (a) but for the 2000 onset. Dates and times are UTC.

2. Data and methodology

The core of the observations used in this study is the Marsyandi meteorological network. This network currently consists of 20 automated observing stations, all equipped with tipping bucket rain gauges, and basic meteorological instrumentation to measure temperature, relative humidity, pressure, wind direction and speed, snow depth, and snow water content. The stations are spaced throughout the Marsyandi region, both on ridges and within river valleys at elevations ranging from 528 m to 4435 m MSL. The network consisted of fewer stations during the 1999 monsoon, but was upgraded to its present status in time for the 2000 monsoon. Given the obvious difficulties involved in maintaining an automated meteorological network in such a remote region, measurement gaps are bound to, and in fact did, occur. Stations affected by significant (greater than 3 days any time prior to 15 September) gaps during the monsoon season are noted in Table 1.

The European, Meteorological Satellites Organization (EUMETSAT) has maintained a geostationary meteorological satellite, *Meteosat-5*, above the Indian Ocean at 63°E since July 1998. This satellite makes visible (VIS), infrared (IR), and water vapor (WV) observations, similar to other geostationary weather satellites like Geostationary Operational Environmental Satellite (GOES), and hourly data for the greater Nepal region (roughly 70°–90° east, 20°–35° north) were used to characterize the time history of weather systems in this study.

The Tropical Rainfall Measuring Mission (TRMM; Kummerow et al. 2000), launched in November 1997, makes passes over Nepal approximately daily. The sensors of interest include the Precipitation Radar (PR), TRMM Microwave Imager (TMI), and the Visible and Infrared Scanner (VIRS). These sensors are described

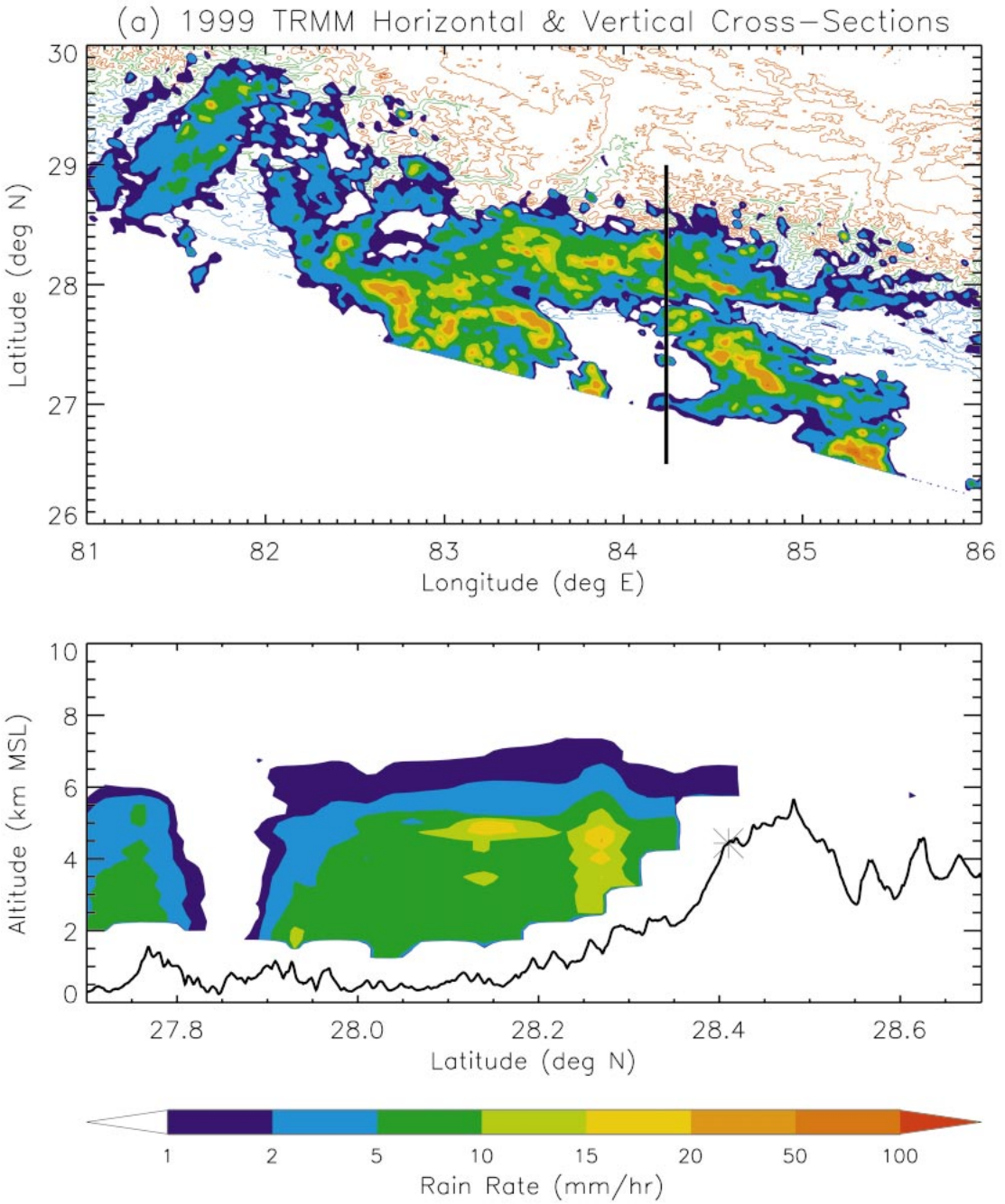

FIG. 3. (a) Horizontal and vertical cross sections of rain-rate estimates from the TRMM PR, at approximately 2220 UTC on 12 Jun 1999. Both cross sections also contain contours of local topography. The black line in the horizontal cross section denotes the longitude along which the vertical cross section is taken. The location of the Rambrong station is marked by an asterisk in the vertical cross section. (b) Same as in (a) except for 2230 UTC on 6 Jun 2000. In the vertical cross sections, note the influence of the coarse digital elevation map used in the 2A25 PR algorithm to avoid surface clutter and sidelobe interference.

in Kummerow et al. (1998). While TRMM does not capture the time history of individual precipitation systems due to its sampling frequency, it was used in this study to characterize the instantaneous spatial (horizontal and vertical) structure of precipitation systems in the Marsyandi region during overpasses.

Twice-daily analyses from the European Centre for Medium-Range Weather Forecasting (ECMWF) were

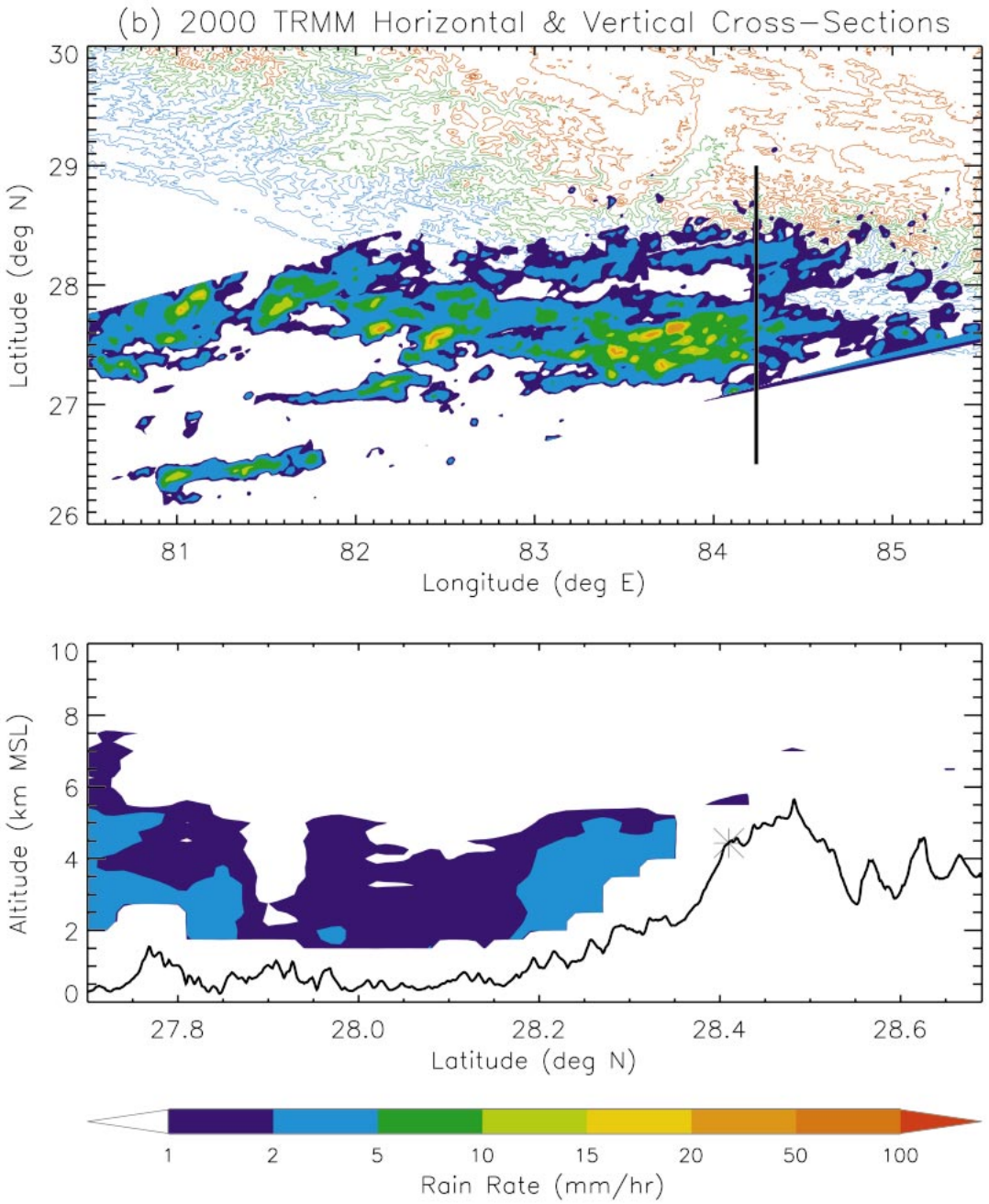

FIG. 3. (*Continued*)

used to understand the synoptic fields associated with the systems observed in this study. These data are on a 2.5° × 2.5° grid. While southern Asia is a relatively data-poor environment, and such a coarse grid precludes the ability to use these data to investigate smaller-scale phenomena, the analyses do provide a basic understanding of what is occurring on the larger scale.

Finally, twice-daily radiosonde data from four stations in India were used to characterize the thermodynamic environment. These stations are relatively far from the Marsyandi network (≈200 km), and the soundings are often fraught with errors (Collins 2000). Nevertheless, they are the only nonmodel thermodynamic information available. The biggest problems encountered with the radiosonde data were clearly identifiable bad values for temperature and dewpoint, and early termination of soundings (defined as soundings that stopped below 200 hPa). Levels with bad data were

TABLE 1. Summary of Marsyandi meteorological network. The 1999 data were originally presented by Barros et al. (2000). JJAS = 1 Jun–30 Sep. Onset rainfall totals are for the heaviest two days.

Station name and number	Type	Elevation (m MSL)	1999 JJAS rain (mm)	2000 JJAS rain (mm)	1999 Onset rain (mm)	2000 Onset rain (mm)
1. Bortung	L	1072	1570	1432	284	183
2. Danfedanda	H	3987	1987	1371*	210	NA
3. Ganpokhara	H	2120	3760	3796	144	87
4. Khudi	L	820	2266	4107	216	110
5. Koprung	H	3133	1564*	3120	205	129
6. Monastery[1]	D	3562	NA	302	NA	113
7. Nargaon[1]	D	4220	NA	339	NA	135
8. Paiyu Khola[1]	L	993	NA	3715	NA	104
9. Pasqam Ridge[1]	H	2950	NA	3503	NA	185
10. Pasqam Village[1]	L	1702	NA	NA	NA	NA
11. Probi[1]	L	1495	NA	3662	NA	124
12. Purano Village	L	1787	NA	3115*	NA	124
13. Purkot	L	528	1482	1079	80	79
14. Rambrong	H	4435	2889	3311	381	462
15. Sundar	H	3823	2882	3226	293	221
16. Syange	L	1200	257*	2372	101	64
17. Tal	L	1358	1266	886*	174	81
18. Tansen	L	1521	1657	1848	324	247
19. Telbrung	H	3168	3467	4343	275	167
20. Temang	D	2760	1181	975	225	140

[1] Added after 1999 monsoon.
* Incomplete record during monsoon.
NA = Not available. Station type = H (high altitude ≥ 2000 m), L (low altitude < 2000 m), D (dry station in lee of Annapurnas).

not considered in the sounding analysis, and appropriate skepticism was used when interpreting these soundings.

3. Observations

a. Small-scale perspective

1) RAINFALL

During the years of 1999 and 2000 negative anomalies in sea surface temperatures existed in the eastern equatorial Pacific Ocean. That is, global circulations were under the influence of the cold or La Niña phase of the ENSO cycle. Based on the aforementioned SOI relationship identified by Shrestha (2000), Nepal would be expected to receive normal to above normal rainfall during these monsoons, and in fact received normal rainfall during both years according to the Nepal Department of Hydrology and Meteorology. During both monsoon seasons neighboring India received normal rainfall as a whole, although the Gujarat region of India experienced drought conditions during both years.

Rainfall totals for 1999 and 2000 JJAS (1 June to 30 September) for each network station are presented in Table 1. Aside from the very large amounts of rain that fell in this region, the most prominent feature is the strong variability. For stations with complete records in 1999, the range was 118–376 cm, a very large difference considering that this difference occurred over a distance of about 25 km (Ganpokhara–Temang). The general pattern in 1999 showed rain totals maximized at higher elevation stations along the ridges.

The rainfall patterns showed some differences in 2000. The biggest change was the near 100% increase in rainfall at Khudi, from 227 cm in 1999 to 411 cm in 2000. Such a large change raises the question of instrument reliability. Checks against manual measurements at the same location, as well as correlation with nearby gauges, indicated that the instrument was operating properly during both years. The cause of this increase is not known—the increase was not associated with any single event, but rather occurred over many events during the monsoon—but could be related to interannual variability manifesting itself at small spatial scales. Rainfall gradients were often stronger in 2000 than in 1999, depending on the stations considered.

Table 1 also shows 2-day rainfall totals for 12–13 June 1999 and 7–8 June 2000. These 2 days were, for most stations, the heaviest rainfall days of JJAS. Moreover, for most stations in either year, the rainfall during these time periods met or exceeded the total rainfall for the prior month of May. These rain events followed about 1 week of little to no rain at the Marsyandi network, and marked the beginning of a period of daily or near-daily rainfall lasting well into September of either year. Therefore, we define these rain events as marking the onsets of the monsoon in central Nepal.

For 8 of 20 stations these 2 days accounted for over 10% of the total rainfall, in one or both seasons. These stations tended to include the highest-altitude ridge stations (Rambrong, Sundar, Danfedanda), dry stations to the north of the Annapurnas (Temang, Monastery, Nargaon), and low-elevation stations further out on the

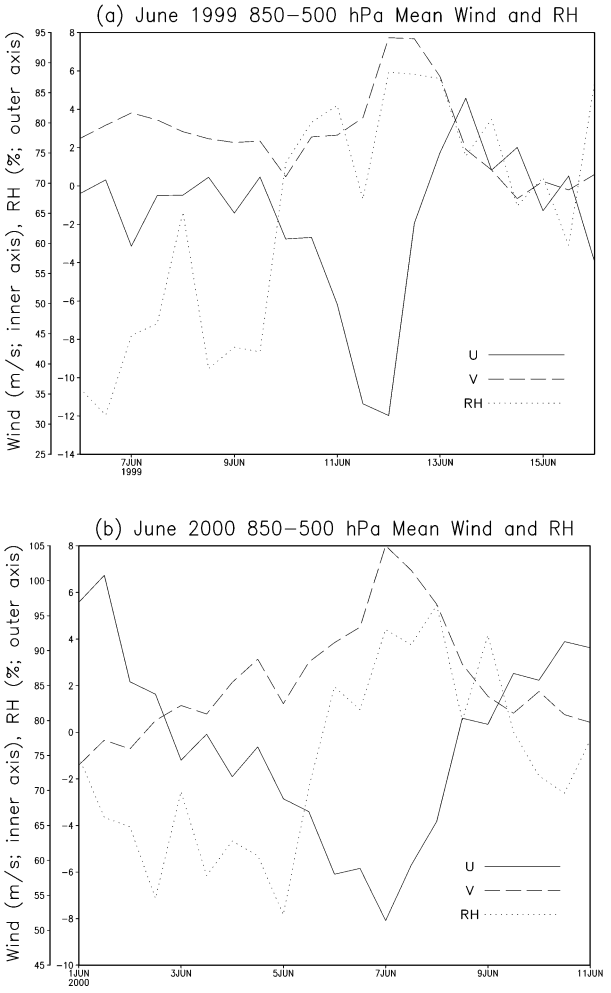

FIG. 4. (a) Time series of ECMWF-analyzed horizontal winds and relative humidity, averaged in the 850–500-hPa layer, at the proxy location for the Marsyandi network (27.5°N, 85.0°E) during early to mid-Jun 1999. (b) Same as in (a) but for early Jun 2000. The zonal wind is denoted by the solid line. The meridional wind is denoted by the dashed line. Relative humidity is denoted by the dotted line. Dates and times are UTC.

plains to the south of the core network (Tansen, Bortung). In fact, some of the northern dry stations received more than one-third of their total monsoon rainfall during the 2000 onset.

In general, the relative spatial distribution of rainfall was similar during both onsets. Rainfall increased with elevation, with some deviations, and the highest elevation station, Rambrong, recorded the most rainfall. The pattern of very large rainfall gradients at the seasonal scale also translated to these shorter time periods associated with the monsoon onsets. As an example of this, during 12–13 June 1999 the Rambrong and Syange stations, separated by only 16.2 km, differ in 2–day rainfall totals by 280 mm, an amount comparable to the *annual* rainfall in the Front Range region of Colorado. The difference was nearly 400 mm in 2000. Despite the similar spatial distributions between the two onsets, the rainfall accumulation during the 2000 monsoon onset at Rambrong was much greater than in 1999, while other gauges generally received 50%–100% more rain during the 1999 onset than in 2000.

Figure 2 shows time series of rainfall for several network gauges for the 1999 (Fig. 2a) and 2000 (Fig. 2b) onsets. The 1999 onset had a strong signal at every gauge, which was consistent with a single, large, long-lived precipitation system. Interestingly, the highest-altitude station, Rambrong (4435 m MSL), dominated many other stations in terms of rainfall intensity, especially early. However, for all gauges 30-min rain rates generally stayed below 30 mm h^{-1}, indicating only light to moderate rain rates even at peak.

The 2000 onset was a longer episode than 1999, covering approximately three days (two heavy days along with a weaker third). Nevertheless, the rain rates tended to be lower than in 1999 except at Rambrong. Unlike the 1999 onset, the main event in 2000 consisted of basically two parts, with a short lull between them. Consistent with its high rainfall total during the 2000 onset (46 cm), Rambrong dominated the other gauges in both intensity and duration of rainfall, although rain rates were similar to 1999. Thus, during both onsets it was duration, rather than intensity, which was responsible for the high rainfall totals. Also, during both onsets intense rain events showed no preferential timing, as opposed to the seasonal average of a nocturnal maximum in rainfall for this region as reported by Barros et al. (2000). This suggests that local mesoscale processes were dominated by large-scale weather.

The relative importance of convective versus stratiform precipitation during these onsets was assessed with the objective of characterizing the morphology of the rain systems. Generally, it is accepted that the intensity of stratiform rain seldom exceeds 10 mm hr^{-1} (e.g., Steiner et al. 1995). But convective rain is not limited to a 10 mm hr^{-1} lower bound. Thus, while we can identify with good confidence convective rainfall when the rain rate is equal to or exceeds 10 mm hr^{-1}, it is much more difficult to classify rain rates below this threshold. In this work, we used both the time series of tip counts at individual gauges and 30-min rainfall accumulations to categorize rainfall during each 30-min period.

First, we calculated the percentage of total rainfall corresponding to long-lived convection (i.e., convection that lasted long enough to produce a significant average rain rate over 30 min) by comparing the rainfall from times when gauge rain rates met or exceeded 10 mm hr^{-1} to the total rainfall. In both years, stations that received the most onset rain (Rambrong, Bortung, Tansen) had by far the largest percentage (>60%) of rainfall from long-lived convection. A significant reduction in percentage of long-lived convective rainfall occurred in 2000 versus 1999; the average among all stations dropped from 46% in 1999 to 19% in 2000. This suggests that long-lived convective

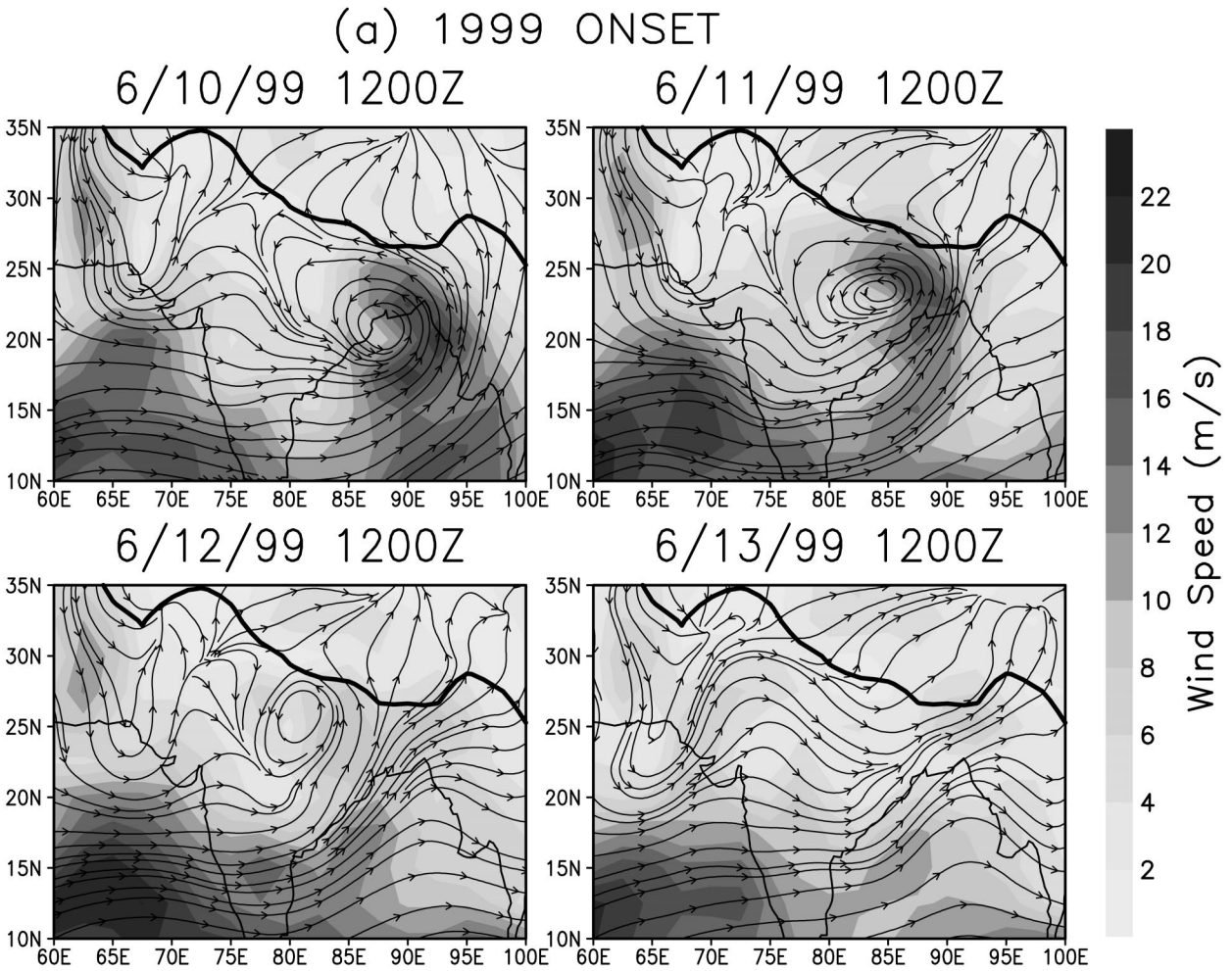

FIG. 5. (a) Time sequence of daily ECMWF analyses, showing 850-mb wind streamlines and speed, starting at 1200 UTC on 10 Jun 1999 (the time of the lowest mean sea level pressure in the Bay of Bengal region). (b) Same as in (a) but starting at 1200 UTC on 5 Jun 2000. The solid black curve denotes the 2000-m elevation contour.

processes were more important for total rainfall during the 1999 onset than in 2000.

Tip data (from the 11 gauges that recorded them) were used to identify 30-min periods that contained short-lived convective rainfall (i.e., convection that did not last long enough to produce a significant average rain rate over 30 min, but that did exceed 10 mm hr^{-1} for a portion of that time). Almost all stations saw at least some short-lived convective rainfall, usually amounting to 25% or less of rainfall totals.

The remaining fraction of unclassified rainfall presumably was either light convective ($R < 10$ mm hr^{-1}) or stratiform rain. This fraction was highest for low-elevation stations that received the least rain during the onsets, as well as for dry stations north of the Annapurnas. It is reasonable to expect that stratiform rain was a significant part of this remaining fraction of rainfall, which for many stations approached or exceeded 50%, and that stratiform rain was present at most gauges during the 1999 and 2000 onsets. Thus, according to the gauges, a mixture of convective and stratiform rain likely was present during the onsets. Convective rain was most important at the gauges that received the most rainfall, whereas stratiform or light convective rain was most important at the gauges that received the least rainfall.

Precipitation structure was investigated further with TRMM–Precipitation Radar (PR) observations of the 1999 and 2000 onsets. Rain rates are well known to vary substantially on very short temporal (<5 min) and spatial scales, particularly in convective situations. Thus, instantaneous measurements of the 4-km TRMM footprint by TRMM will not necessarily represent the 30-min measurements at the rain gauges. Although the PR products underestimate rainfall rates in this region (e.g., Barros et al. 2000), they provide the only means to examine the vertical structure of precipitating systems and storm morphology in this region of the world.

The TRMM satellite passed over the Marsyandi network around 2220 UTC on 12 June 1999. This was immediately after the main peak in rainfall at most gaug-

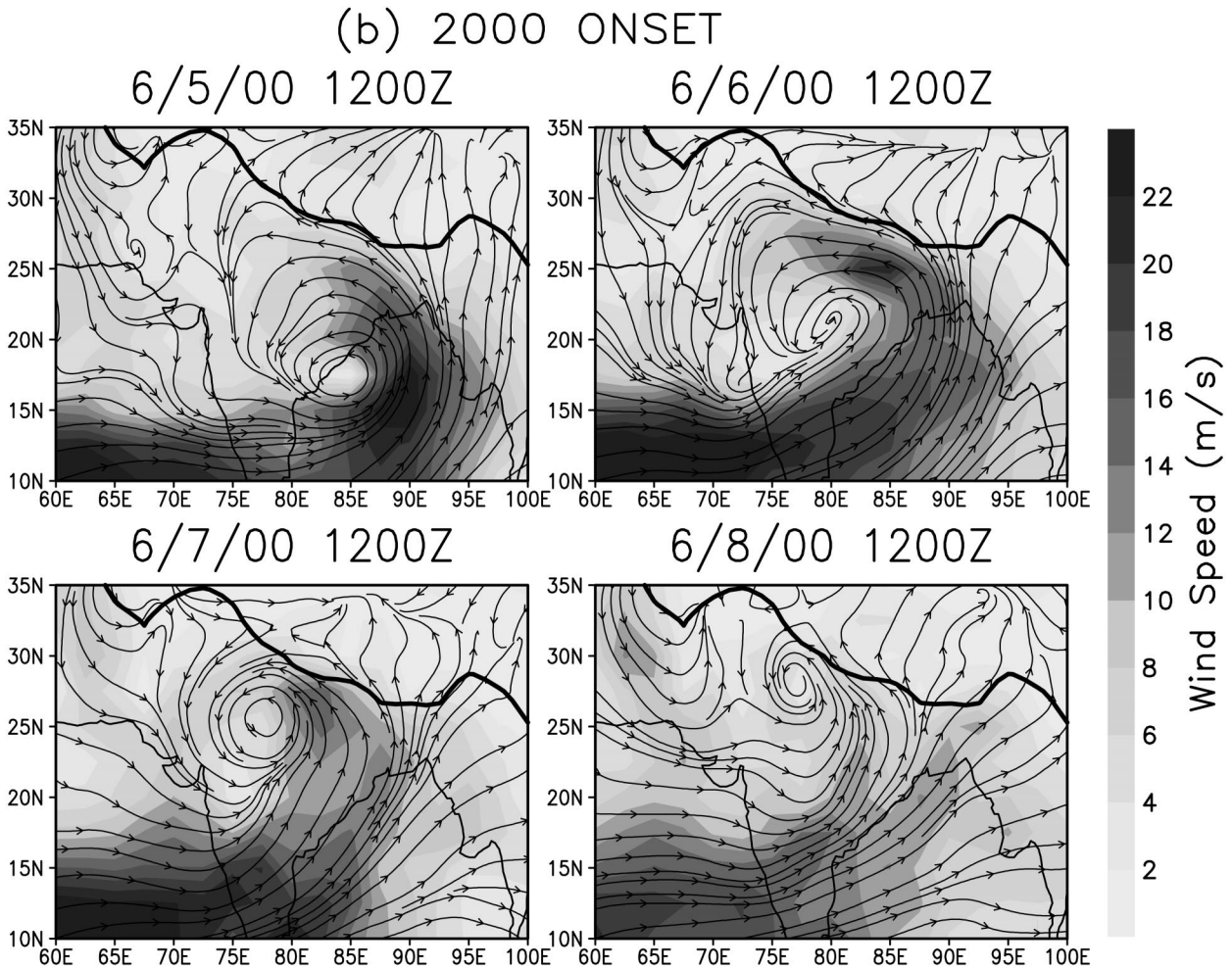

FIG. 5. (*Continued*)

es. Figure 3a illustrates PR horizontal and vertical cross sections of rain estimates in the Marsyandi region. The data show a number of convective cores in the region, but at this time the heaviest rains were not occurring at network stations, consistent with the fact that this was past the time of peak gauge rainfall. The convective cores were embedded within a large region of light rain (<5 mm hr^{-1}). The vertical profile of PR rain data shows what appeared to be shallow stratiform rain at the network, which was almost completely located within the light rain region at this time.

In 2000, the TRMM satellite passed over the Marsyandi network around 2230 UTC on 6 June. Figure 3b shows PR rain estimates for this time, which was after a major peak in rainfall at Rambrong. Again, heavy rains were not occurring at the network, consistent with the low observed gauge measurements around this time (generally under 10 mm h^{-1}). The region was being affected by light rain, with some embedded convection to the south. Like 1999, the vertical cross section depicts shallow stratiform rain at the network.

Data from the Visible and Infrared Scanner and the TRMM Microwave Imager aboard the TRMM satellite were also examined. The VIRS observations and the TMI brightness temperature fields support the PR observations during both onsets, and were consistent with the presence of deep convection in the area, but not at the network gauges during the overpasses. Overall, the TRMM data reveal that the onsets storms were characterized by a mixture of convective and stratiform rain, mainly in the form of embedded convection within a larger area of light rain, which encompassed much of the Marsyandi region. This inference is consistent with the gauge data.

2) WINDS

Figure 4 shows 850–500-hPa averaged U and V winds, along with average relative humidity in the same layer, as functions of time at a grid point (27.5°N, 85.0°E) close to the Marsyandi network, for both the 1999 and 2000 onsets. An increase in easterly wind

strength concurrent with increases in southerly flow and relative humidity occurs in both years around the time of the onset of continuous rain at the network (~0600 UTC on 11 June 1999, after 0600 UTC on 6 June 2000).

Comparing Figs. 2 and 4, southerly (upslope) flow in the 850–500-hPa layer continued throughout the rain event in the vicinity of the network, and the termination of rain and moist (RH > 70%) upslope flow were largely coincident. The role of moist, synoptic-scale upslope flow in enhancing convection due to an influx of low-level moisture and lifting of conditionally unstable air has been noted in other parts of the world, such as the Front Range of Colorado (e.g., Doswell 1980). This mechanism is consistent with our analysis along the south slopes of the Himalayas.

3) THERMODYNAMIC ENVIRONMENT

There are four radiosonde stations in India that are relatively close to the network. From these stations, the soundings immediately prior to the onset of sustained rains at the Marsyandi network were examined for each onset, as these soundings represent the best chance to sample the prestorm environment. (This worked out to be 1200 UTC on 11 June 1999 and 1200 UTC on 6 June 2000.) In 1999, the average CAPE for surface mixed layer (i.e., lowest 50 hPa) parcels was 439 J kg^{-1}. (Parcels taken from higher altitudes—925–850 hPa—contained lower CAPE values.) Average precipitable water was estimated to be 56.2 mm. In 2000, the average CAPE was 1484 J kg^{-1}, and the average precipitable water was 59.4 mm.

Despite the low CAPE observed in 1999, the sounding data from both onsets are still consistent with the prodigious rainfall observed. In 1999, all of the soundings from the 1999 onset contained potentially unstable layers, so any large-scale lifting should have led to further destabilization as the air mass approached the network region and those layers were lifted and cooled (e.g., Barros and Kuligowski 1998). Also, during both years CAPE values either grew to (1999) or were sustained at (2000) more than 1000 J kg^{-1} during subsequent days.

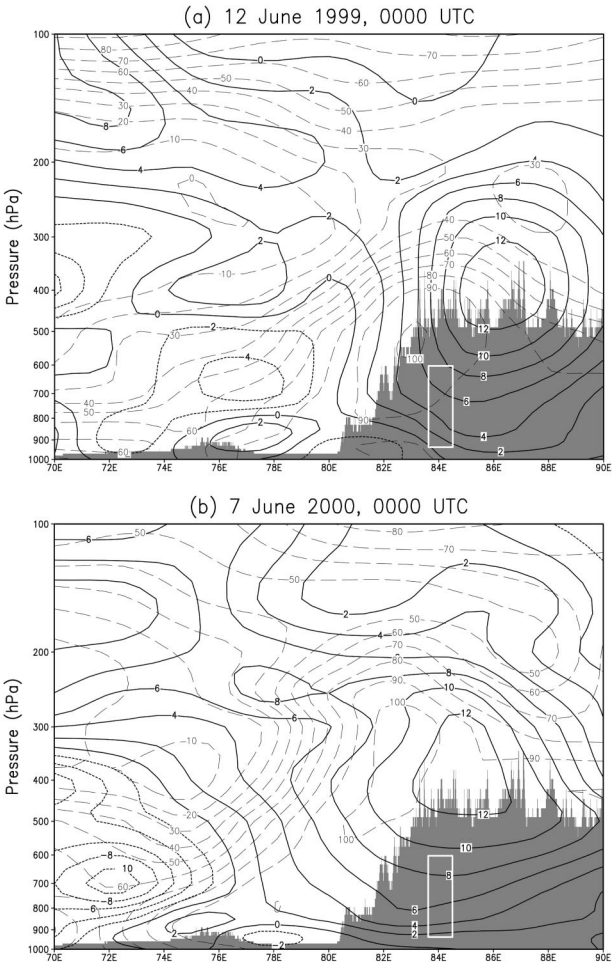

FIG. 6. (a) Longitude–height analysis at 27.5°N for 0000 UTC on 12 Jun 1999. (b) Same as in (a) but for 0000 UTC on 7 Jun 2000. Shown are meridional wind component [V, solid contours positive/southerly, short-dashed contours negative/northerly, (m s^{-1})] and relative humidity [dashed contours, (%)]. The gray shading shows maximum elevation achieved by the terrain between 27° and 30°N. The white box denotes the approximate range of network station locations projected onto the plane.

b. Large-scale perspective

Now that the local aspects of the 1999 and 2000 onsets in central Nepal have been examined, it is important to investigate how they relate to the larger scale. That is, we need to determine what synoptic weather systems were responsible for the rainfall observed during these onsets, as well as understand how the onsets in central Nepal fit within the evolution of the whole Asian monsoon system.

1) SYNOPTIC OVERVIEW

Figures 5a and 5b show a sequence of wind streamlines and speeds at 850 hPa over the expanse of south Asia during the time period associated respectively with the 1999 and 2000 monsoon onsets in central Nepal. During both onsets, a low pressure system (hereafter termed monsoon depression) developed in the Bay of Bengal, and then proceeded northwestward toward the Himalayas. The 2000 depression formed southwest of the 1999 genesis location, and that resulted in its track being to the west of the 1999 depression. The arrival of both depressions at the mountains coincided with the onset of moist upslope flow and the beginning of rain at the network, as the southerly to southeasterly flow on their northeastern flanks impacted the Himalayas.

This effect is elucidated in Figs. 6a–b, which show longitude–height cross sections (at 27.5°N) of meridional wind and relative humidity at 0000 UTC on 12

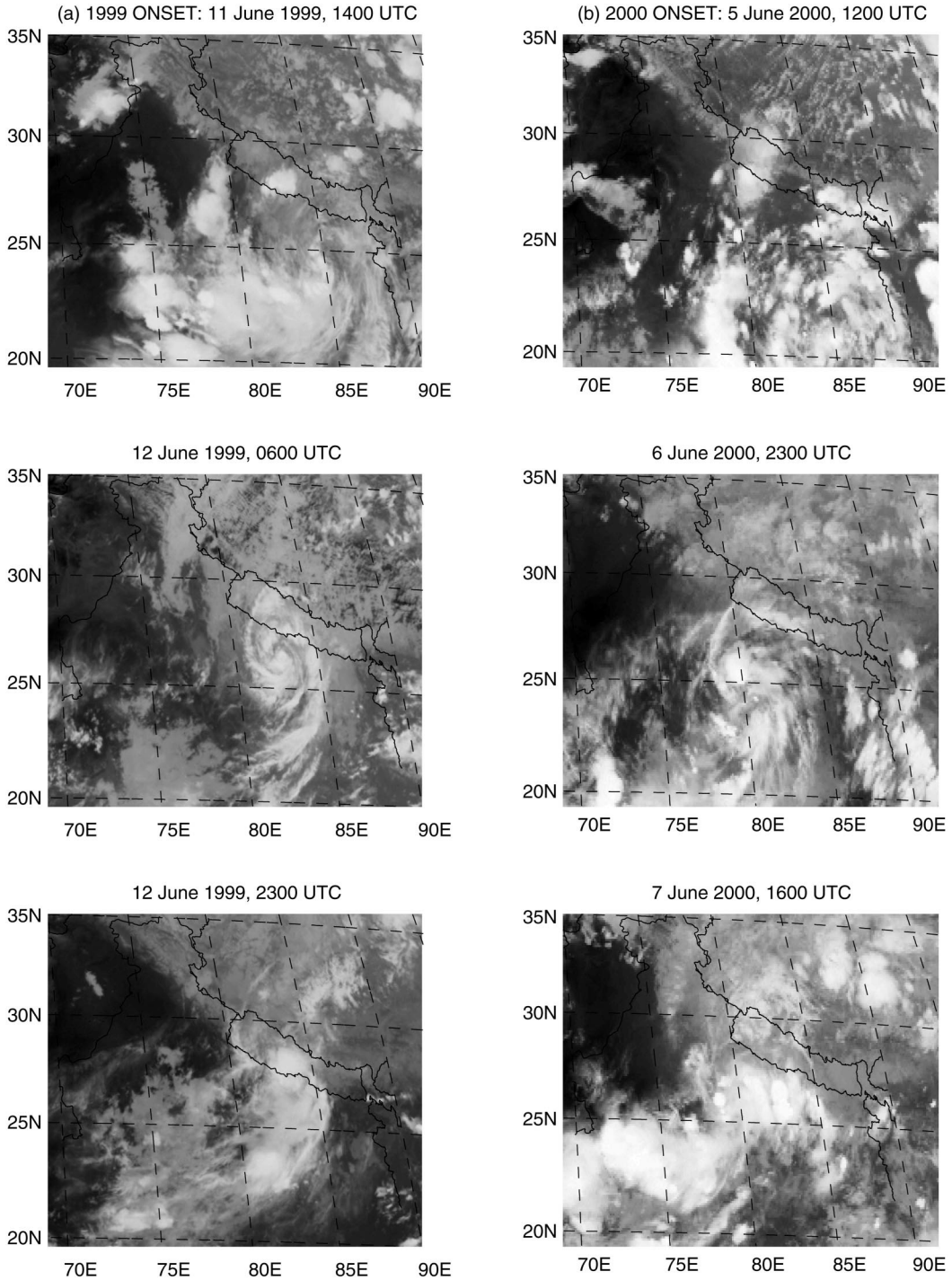

FIG. 7. IR images from *Meteosat-5*. (a) 1999: 1400 UTC 11 Jun, 0600 UTC 12 Jun, and 2300 UTC 12 Jun (coincident with the TRMM overpass in Fig. 3a). (b) 2000: 1200 UTC 5 Jun, 2300 UTC 6 Jun (coincident with the TRMM overpass in Fig. 3b), and 1600 UTC 7 Jun.

June 1999 (Fig. 6a) as well as at 0000 UTC on 7 June 2000 (Fig. 6b). The eastern flank of the monsoon depressions created southerly midlevel jet structures in the eastern third of the domain as the depressions encroached upon the mountains. The network region resides in the lower quadrant of this jet. For either year, the jet was responsible for substantial moisture flux toward the Marsyandi network, and its evolution and decay mirrored the onset and termination of rain at the network.

2) Relationship to the Asian monsoon

ECMWF analyses for May and June of both years revealed that these depressions followed the development of the monsoon onset vortex in the Arabian Sea, and occurred when the Somali jet was well developed. These two events typically precede the onset of monsoon rains over SW India (Krishnamurti et al. 1981). In 1999, a vortex appeared in the Arabian Sea around mid-May, followed in late May by a weak low pressure system in the Bay of Bengal, which propagated northeastward over Bangladesh. The next low pressure system was the depression responsible for the onset of the rainy season in Nepal. In 2000 there was an Arabian Sea vortex that formed in late May. The subsequent depression formed in the Bay of Bengal was responsible for the 2000 monsoon onset in Nepal. In both years the depressions were associated with increased low-level westerly flow over much of the Indian subcontinent (see Fig. 5), suggesting that the Nepal onset occurred as the Indian monsoon was developing and spreading northward. Indeed, the paths of the 1999 and 2000 depressions brought them over northern India, linking the onsets in central Nepal and northern India by the passage of these storms.

This link between the two regions is demonstrated by *Meteosat-5* imagery. Figure 7 shows a sequence of *Meteosat-5* IR images for the 1999 (Fig. 7a) and 2000 (Fig. 7b) onsets. For 1999, the imagery shows convective activity associated with the trajectory of the depression after leaving the Bay of Bengal, then crossing northern India, and finally crashing into the Himalayas in the vicinity of the network. At first, widespread convection associated with this system existed over much of northern India. However, as the storm approached the mountains its convection became more organized and localized, and rotation was more apparent. (Note the classic spiral arm structures overrunning Nepal at 0600 UTC on 12 June.) However, the convective organization clearly decayed as the system collided with the mountains (2300 UTC on 12 June—roughly coinciding with the 1999 TRMM overpass, Fig. 3a), and convection in the region took on a more disorganized appearance.

For 2000, the imagery shows somewhat disorganized convection associated with the monsoon depression approaching the mountains from the southeast, again crossing northern India, although its track was situated west of the 1999 track. Like 1999, as the storm approached the mountains the convection appeared to organize and spin up. By 2300 UTC on 6 June 2000, there is a distinctive vortex structure, complete with spiral arms. One of the spiral arms extended to the middle Himalayan region in the vicinity of the network (nearly coincident with the 2000 TRMM overpass, Fig. 3b), although the main convection did not impact the Marsyandi region as in 1999. The organized vortex structure did not last long, as the system quickly devolved and

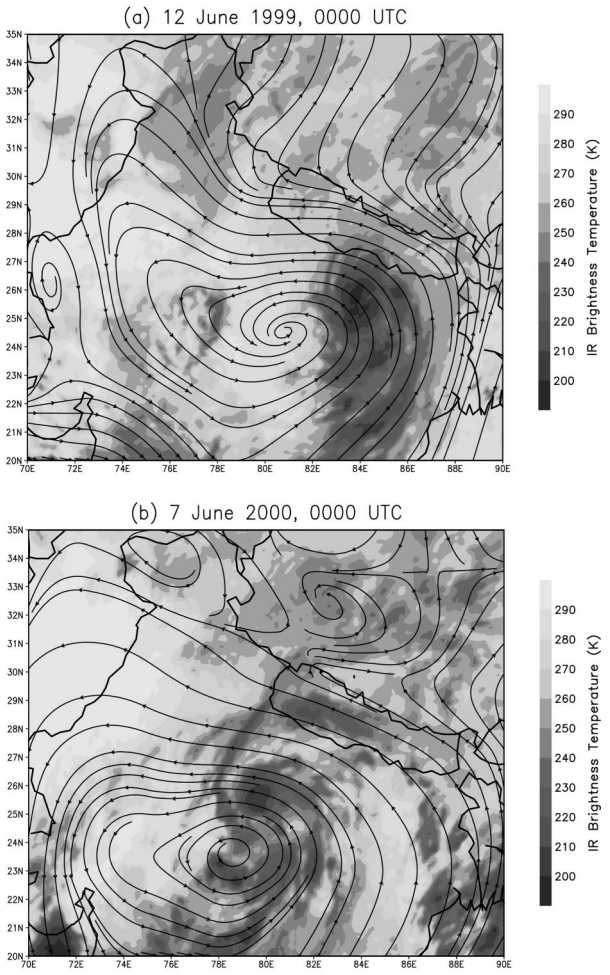

FIG. 8. (a) ECMWF 850-mb wind streamlines and *Meteosat-5* IR satellite brightness temperatures for 0000 UTC 12 Jun 1999. (b) Same as in (a) but for 0000 UTC on 7 Jun 2000.

spawned widespread convective clouds across northern India and Nepal.

The increasing convective organization and rotation as the systems approached the mountains calls for further analysis. Overlays of satellite and ECMWF data revealed that this region of organized convection actually existed in the northeastern quadrant of the main depression, in the southerly to southeasterly flow (Figs. 8a–b). This is contrary to the climatology of monsoon depression structure with convection predominant in the SW quadrant (e.g., Das 1987). Both of these depressions exhibited a similar structure earlier in their lifetimes, with convection focused near their core and SW quadrant. It was only at later times, as the depressions encroached upon the Himalayas, that the convective activity shifted to the northeastern flank and became organized. This phenomenon is examined in more detail in the next section.

The ECMWF analyses and Meteosat data suggest an explanation for the 33%–50% decrease in rainfall from

1999 to 2000, as well as for the increased convective rainfall fraction observed in 1999, which relates to the trajectories of the monsoon depressions after landfall. The 2000 depression's track was situated west of the 1999 track. Consequently, the main convection on the northeastern flank of the depression impacted the network area in 1999 (visible in the TRMM-PR image, Fig. 3a), but only grazed this area with rainbands on its periphery in 2000 (one of which is visible in the TRMM-PR image, Fig. 3b). The tracks of the monsoon depressions critically affected how much rain fell during both onsets, and they are therefore a critical element of the interannual variability of rainfall in central Nepal.

3) STORM TRACKS

According to the climatology, monsoon depressions from the Bay of Bengal are known to travel in the west-northwest direction along the seasonal monsoon trough that resides over northern India (e.g., Das 1987). The depressions associated with the central Nepal onsets in 1999 and 2000 moved more northwestward than to the W or WNW, and demonstrated substantial convective organization even as they arrived near the Himalayas. Das (1987) notes that monsoon depressions sometimes move northward, especially late in their life cycle. In addition, Potty et al. (2000) reported on a modeling study of four monsoon depressions, one of which traveled almost due north over central India. ECMWF analyses from the years 1997–2001 suggest that northwestward propagation is not at all unusual, at any point in the monsoon season. Thus, the motion of the 1999 and 2000 depressions is not unique, but their motion along with their increasing convective organization are very interesting.

When the 2000 depression formed, the eastern edge of the surface monsoon trough that normally resides over northern India was oriented slightly more to the south than the monsoon trough at the time of the 1999 depression. As is typical with monsoon depressions (e.g., Das 1987), both systems formed on the eastern edge of this trough, so this accounts for the difference in depression genesis locations between the two onsets. Both depressions moved within the monsoon trough.

Many studies examining the motion of monsoon depressions have used the concept of vorticity balance (Rao and Rajamani 1970; Krishnamurti et al. 1976; Douglas 1992). The general conclusion has been that these systems follow low-level vorticity generation by convergence on their western flank. Using the ECMWF data, each component of the vorticity equation (horizontal and vertical advection, divergence, and tilting) was calculated during the 1999 and 2000 depressions. Figure 9a shows the observed vorticity tendencies at 1200 UTC on 10 June 1999 and at 1200 UTC on 5 June 2000, as the depressions were making landfall. Also shown is the calculated vorticity tendency (horizontal advection and divergence only) for both storms. (The magnitude of vertical advection and tilting contributions was very small and was neglected.)

While the observed and calculated vorticity tendencies do not match completely, likely due to subgrid-scale processes such as convection, the analysis shows a clear preference for the NW flank of the depression, which appears to explain the observed motion direction. The horizontal advection of vorticity and the generation of vorticity by convergence were consequences of the wind speed maximum on the NE flanks of these storms (see Fig. 5). This speed maximum is a common feature of monsoon depressions (Rao 1976; Potty et al. 2000). The enhanced convergence on the NW flank is hinted at in Fig. 5, with the deceleration of the flow as it wrapped around the north of each depression. Horizontal advection was most important on the NE flank, where wind speeds were largest. Both storms were traveling to the NW, so wind speeds on the NE flank should be greater than elsewhere since storm motion and storm-relative winds would reinforce each other in that quadrant, and thus maintain the existing direction through vorticity advection and convergence. However, based on tracking the 850-hPa vorticity maxima in the ECMWF data, the 1999 storm averaged a speed of less than 4.5 m s^{-1}, and the 2000 storm's speed was less than 6 m s^{-1}. This is not always enough to resolve the observed discrepancy between wind speeds in different quadrants, particularly at 1200 UTC on 11 June 1999 and at 1200 UTC on 6 June 2000 (Fig. 5).

To assess the potential for blocking to occur, crude estimates of the Froude number (Fr) were calculated for these flows using ECMWF data. Taking a difference of potential temperature $\Delta\theta = 30$ K between mountaintops and low elevations ($\Delta H \cong 5000$ m), a reference value of $\theta_0 = 300$ K for the potential temperature at low elevations, and a low-level wind speed U = 10 m s^{-1}, the Froude number is 0.14 [$\mathrm{Fr} = U/(g\,\Delta\theta\Delta H/\theta_0)^{1/2}$], which suggests that the low-level flow was blocked by the mountains in both cases. Given the observed instability during the 1999 and 2000 onsets, this result would not apply universally as parcels could be lifted over mountains by convective processes, but it is a good first-order approximation for large-scale flow.

Therefore, as the monsoon depressions leave the Bay of Bengal and move over northern India, the Himalayan range acts as a boundary barrier impeding the flow. The Coriolis acceleration along the mountains vanishes, the pressure gradient normal to the mountains increases, and the along-mountain (easterly) flow is strengthened. Geostrophic adjustment of the monsoon vortex leads to an increase of the absolute angular velocity and centripetal accelerations, thus increasing convergence and cyclonic circulation consistent with the time evolution of these depressions in the infrared imagery (Figs. 7a–b). Because the mountains do not form a uniform obstacle to flow, another form of flow adjustment is to increase shear in response to changes in topography. Nonlinear effects due to the spatial variation of terrain features

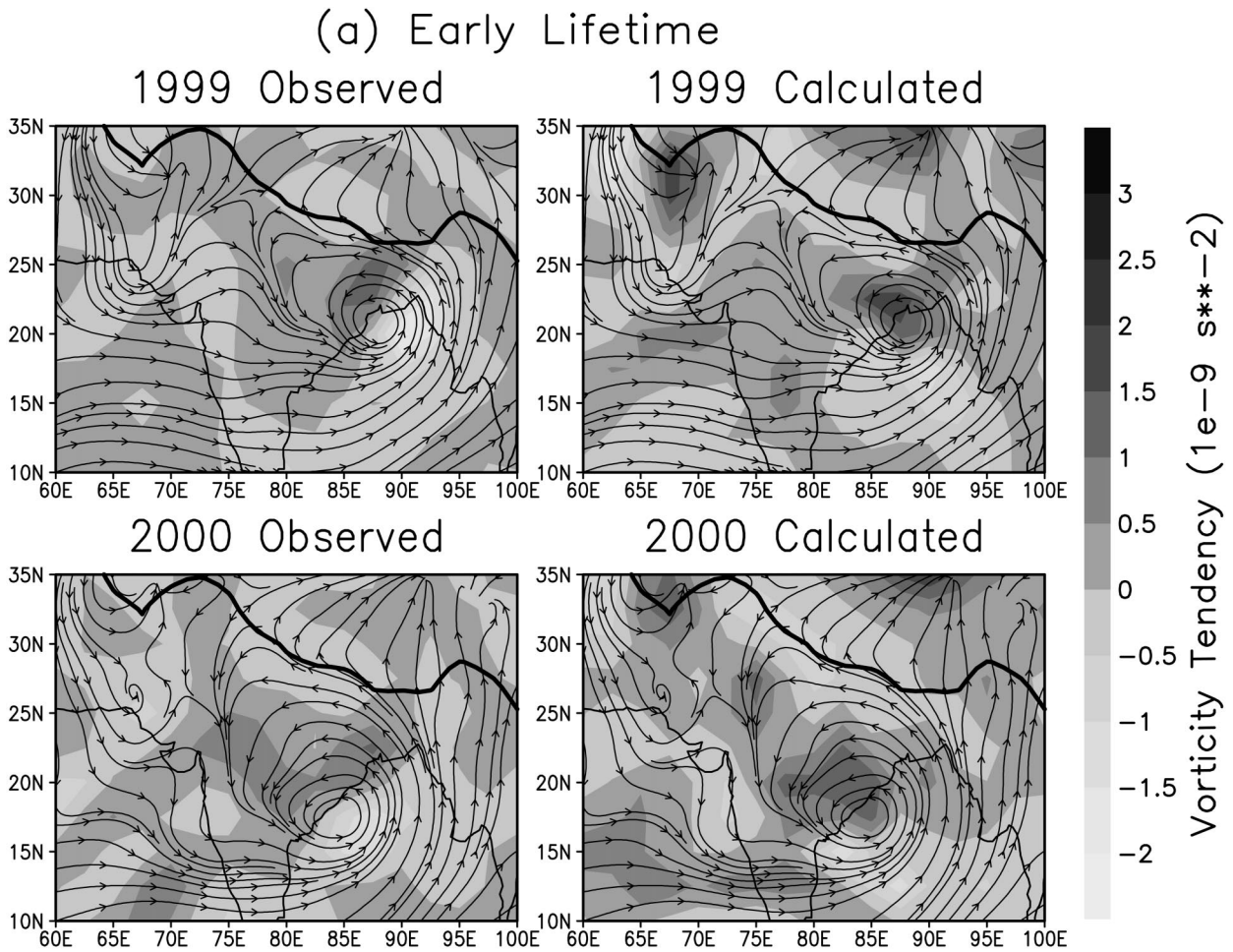

FIG. 9. (a) Observed vorticity tendencies for 1200 UTC 10 Jun 1999 and 1200 UTC 5 Jun 2000. Also shown are calculated vorticity tendencies, due to horizontal advection and divergence, for both storms. (b) Same as in (a) but for 0000 UTC 12 Jun 1999 and 0000 UTC 7 Jun 2000.

add complexity to the flow and establish preferential regions of updrafts, which can develop into deep convective cells embedded in the spiral arms of the depression (Gill 1982).

Furthermore, the ECMWF data show low-level cold advection, on the order of several kelvins per day, occurring on the northern flanks of these storms initially. We compare the low-level southeasterly flow to a density current that is colder, and thus denser, than its environment. Blocking of this cold current would contribute to a further increase of the pressure gradient force, accelerating the westward flow along the mountain range, and accentuating the jetlike structure in the northeastern flank of the vortex (Bluestein 1993). These mechanisms are consistent with the observed speed increase on the northeastern flanks of the depressions, especially at times like 1200 UTC on 6 June 2000 (Fig. 5b). Over time friction and latent heat release through precipitation should work to steadily erode the potential energy of the vortex, decelerating the flow, particularly as the depressions got closer to the Himalayas. Thus, the jetlike features should weaken late in the storms' life cycles, as observed.

The agreement between calculated and observed vorticity tendencies did not hold up throughout the duration of the onset storms. Figure 9b shows observed and calculated vorticity tendencies for 0000 UTC on 12 June 1999 and 0000 UTC on 7 June 2000. This is late in the storms' lifetimes, when convective organization and rotation on their northeastern flanks were near maximum. While the observed vorticity tendencies show the storms propagating mostly northward at this point, the calculated tendency is for increasing vorticity on the northeastern flanks. This was almost entirely due to generation by convergence, as the southerly winds on this flank steadily slowed down. As a result of blocking by the Himalayas, the winds in this sector decelerate over time, so that upstream convergence occurred. This region coincides with the area covered by the intense, organized convection in the satellite imagery (Figs. 8a–b).

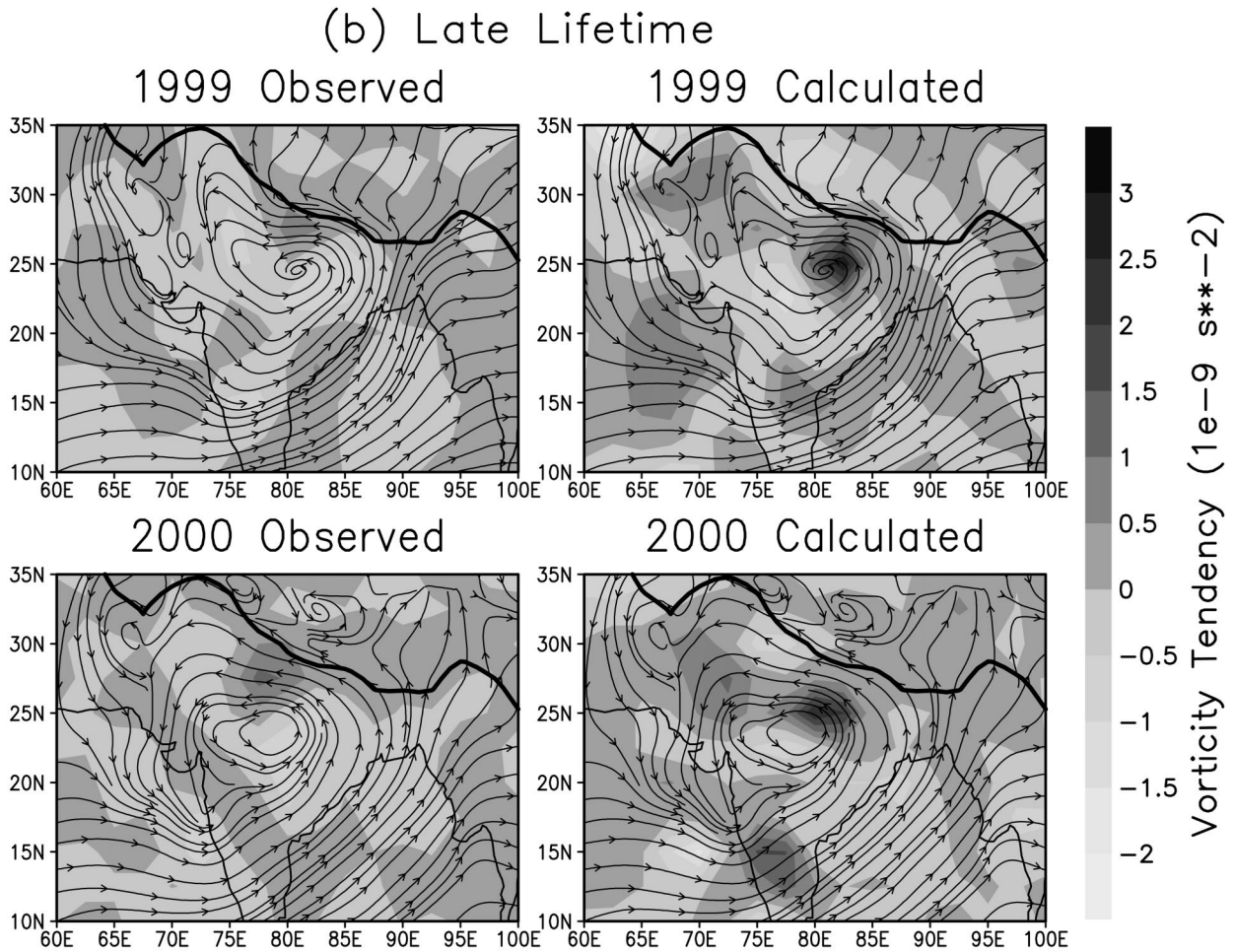

FIG. 9. (*Continued*)

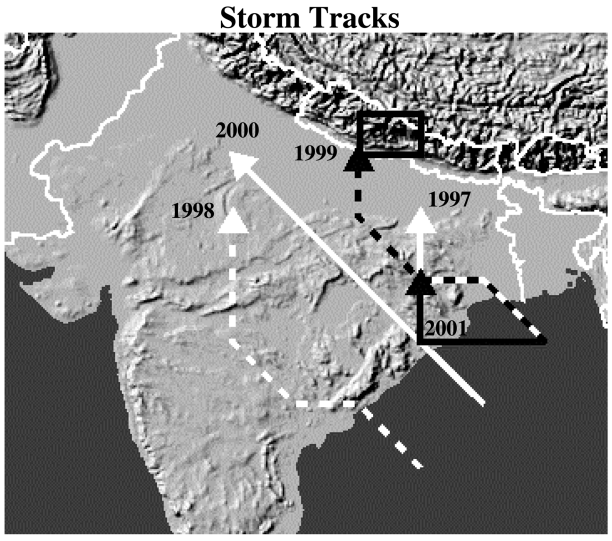

FIG. 10. Storm tracks for the Nepal onset depressions (1997–2001). Tracks were determined by the locations of the 850-mb relative vorticity maxima in the ECMWF data. The black box shows the relative location of the Marsyandi network.

It is also a region of positive advection of moisture and warm temperatures, which should work in concert with the vorticity generation to assist in the development of organized convection. Thus, while the ECMWF data are too coarse to resolve any mesoscale vortex generation or convective enhancement on the northeastern flanks, they do provide evidence for why they occurred, even as the depressions overall weakened, filled, and continued to the northwest.

A strong interaction of the seasonal cycle and the 30–60-day global-scale intraseasonal oscillation (ISO; Madden and Julian 1972) with the onset of the Asian summer monsoon was found by many investigators (Murakami et al. 1986; Chen et al. 1988; Kuma 1988; Wang and Xu 1997; Wu et al. 1999). Krishnamurti and Subrahmanyam (1982) showed that the northward-propagating portion of this mode can be associated with the development of cyclonic storms in both the Arabian Sea and Bay of Bengal. Given the timing of the 1999 and 2000 monsoon depressions, it is possible that the ISO played a role in their development, as well as their northward propagation. However, the ECMWF data were not time-

filtered to examine this possibility in detail, and no obvious northward motion of vorticity, etc. prior to the development of the depressions was observed in the unfiltered data. In 2001, the depression responsible for the monsoon onset in Nepal (discussed later) developed out of a northward-propagating vorticity maximum, which traveled from near the equator into the Bay of Bengal. However, the subsequent depression traveled initially *westward*, only turning north several days later. Thus, if this vorticity maximum was associated with the ISO, then it does not appear that the ISO plays a critical role in causing northward propagation of monsoon depressions, at least during 2001.

The influence of storm tracks on onset rainfall is further investigated by an exploratory analysis of central Nepal monsoon onsets in other years (1997, 1998, and 2001). Nepal Department of Hydrology and Meteorology (DHM) daily rainfall data from gauges in the vicinity of the Marsyandi network (1997–1999), Marsyandi network data from June 2001, as well as ECMWF objective analysis data for 1997, 1998, and 2001 were used. The data revealed that early monsoon depressions in the Bay of Bengal also played important roles in the onsets of those years in Nepal, though onset rainfall totals were not as dramatic as 1999 and 2000. While some gauges received comparable rainfall to 1999 and 2000, the breadth of high rainfall totals from those years was not observed in 1997, 1998, or 2001.

Storm tracks for all five depressions are shown in Fig. 10. The 1997 depression formed near where the 1999 depression formed, in the head of the Bay of Bengal. It was about as strong as the 1999 and 2000 depressions but it moved more northward than the 1999 depression, and affected the Himalayas more to the east of the Marsyandi network. The 1998 depression formed south of the 2000 depression and was the weakest of the five. By the time its long trek brought it near the mountains, the resulting southerly flow was significantly weaker than in 1999 or 2000. The 2001 depression formed near the 1997 and 1999 genesis locations, but moved very slowly westward. Based on vorticity advection estimates, its movement probably was impeded by very strong low-level westerlies over India. While the monsoon onset was difficult to detect in the 2001 rainfall data, data from radiosondes launched near the Marsyandi network revealed that the appearance of the monsoon depression was concurrent with a strengthening of southerly to southeasterly winds and an increase in moisture throughout the depth of the troposphere. These radiosondes were launched as part of the Monsoon Himalayan Precipitation Experiment (MOHPREX), which occurred during June 2001. Note that the depressions from 1997, 1998, and 2001 all had some northward component to their motion. Vorticity analyses revealed similar processes to 1999 and 2000 at work.

In all of these cases (1997, 1998, 2001), the tracks of the monsoon depressions, as well as their intensity, precluded the strong southerly flow over the Marsyandi network observed in 1999 and 2000. The tracks also precluded northward advection to the Marsyandi of convection that may have existed on the depressions's eastern flanks. Correspondingly, onset rainfall was not as dramatic as 1999 and 2000, although there was an increase in rainfall during each depression's lifetime, and this increase heralded the arrival of regular rainfall in the subsequent days and weeks (i.e., the monsoon).

4. Discussion and conclusions

This study focused on a meteorological network that was established in the Marsyandi River basin in central Nepal. This region shows extremely large gradients in rainfall over small spatial scales (10–20 km), on the timescales of both the monsoon season as well as individual weather events. The local and large-scale aspects of the 1999 and 2000 monsoon onsets in this region have been described and explained through a variety of observations.

The onsets manifested themselves in the form of heavy, multiday rain events, which then heralded the arrival of subsequent daily/near-daily rainfall for the rest of the summer season. The rain events were synchronized with a regional wind shift to moist, conditionally unstable, southeasterly upslope flow. The rain systems consisted of broad areas of stratiform rain with embedded convection. The large variability in rain totals was the result of variability in convective activity; rain gauges with larger fractions of convective rainfall generally received the most rain, and vice versa. Large-scale circulations likely set the stage for high precipitation accumulations. But small-scale and mesoscale circulations, affected by the local topography and unresolved by the ECMWF analyses used here, probably played key roles in actually realizing the heavy rains from convection, and determining which gauges received the most rain.

Through an examination of the large-scale conditions, it was determined that Bay of Bengal monsoon depressions were the proximate cause of the onsets in central Nepal. These depressions occurred very early in the season, as the Indian monsoon was strengthening and spreading northward. The most relevant features of these depressions were the enhanced winds on their northeastern flanks, in response to storm motion and blocking by the Himalayas. These winds provided moist upslope flow in central Nepal, and the convergence caused by their eventual deceleration led to the development of organized convection in this region.

The track of the 1999 depression made much of this eastern flank convection collide with the Himalayas in central Nepal, rather than just graze the area as in 2000. This caused rainfall totals in 1999 to exceed those in 2000 by large margins (50%–100%), and accounted for the higher fraction of convective rainfall in 1999. While both storms moved in roughly the same direction, the 2000 storm formed further SW than the 1999 storm,

which explained why its track was situated west of the 1999 depression. The importance of depression strength and motion track for onset rainfall in central Nepal was supported by a preliminary analysis of the monsoon onsets of 1997, 1998, and 2001, which also featured Bay of Bengal depressions.

Climatological maps of monsoon onset dates over Nepal and India (e.g., Das 1987) reveal that the onsets over central Nepal and much of northern India are relatively coincident, normally occurring in the period 10–15 June. The results of this study suggest that the specific mechanism for this linkage is an early Bay of Bengal monsoon depression. The heavy rains near the core of this depression affect northern India, while moist upslope flow and rain on its eastern flank affect central Nepal. Albeit a relatively short record of 5 yr (1997–2001), the data analyzed here suggest that the monsoon onset in central Nepal is closely linked to monsoon depressions in the Bay of Bengal.

Furthermore, because similar depressions form throughout the monsoon season [typically two per month (Saha et al. 1981)], very active phases of the central Nepal monsoon may be related to the occurrence of monsoon depressions in the Bay of Bengal, depending on the specific tracks taken by those depressions. Accordingly, any reduction in the frequency of those depressions, as can occur during ENSO (Chen and Weng 1999), could have an impact on seasonal rainfall totals.

Acknowledgments. The authors would like to thank the Nepal Department of Hydrology and Meteorology for their generous cooperation and assistance with this research. Dr. Jaakko Putkonen maintains the Marsyandi network and helped with the compilation of station data. Tank Ojha assisted with network construction and maintenance. *Meteosat-5* data were obtained from SSEC at the University of Wisconsin. TRMM data were obtained through the NASA Goddard Space Flight Center DAAC. ECMWF analyses and Indian radiosonde data were obtained through the NCAR Mass Storage System. This research and the Marsyandi network are being supported by NASA/TRMM through Grant NAG5-7781, and by NSF under Award EAR-9909498.

REFERENCES

Barros, A. P., and R. J. Kuligowski, 1998: Orographic effects during a severe wintertime rainstorm in the Appalachian Mountains. *Mon. Wea. Rev.,* **126,** 2648–2671.

——, M. Joshi, J. Putkonen, and D. W. Burbank, 2000: A study of the 1999 monsoon rainfall in a mountainous region in central Nepal using TRMM products and rain gauge observations. *Geophys. Res. Lett.,* **27,** 3683–3686.

Bluestein, H. B., 1993: *Synoptic-Dynamic Meteorology in Midlatitudes.* Vol. II, *Observations and Theory of Weather Systems,* Oxford University Press, 594 pp.

Chen, T.-C., and S.-P. Weng, 1999: Interannual and intraseasonal variations in monsoon depressions and their westward-propagating predecessors. *Mon. Wea. Rev.,* **127,** 1005–1020.

——, R. Y. Tzeng, and M. C. Yen, 1988: Development and life cycle of the Indian monsoon: Effect of the 30–50 day oscillation. *Mon. Wea. Rev.,* **116,** 2183–2199.

Collins, W. G., 2001: The operational complex quality control of radiosonde heights and temperatures at the National Centers for Environmental Prediction. Part II: Examples of error diagnosis and correction from operational use. *J. Appl. Meteor.,* **40,** 152–168.

Das, P. K., 1987: Short- and long-range monsoon prediction in India. *Monsoons,* J. S. Fein and P. L. Stephens, Eds., John Wiley & Sons, 549–578.

Dhar, O. N., and P. R. Rakhecha, 1981: The effect of elevation on monsoon rainfall distribution in the central Himalayas. *Monsoon Dynamics,* J. Lighthill and R. P. Pearce, Eds., Cambridge University Press, 253–260.

Doswell, C. A., III, 1980: Synoptic-scale environments associated with high plains severe thunderstorms. *Bull. Amer. Meteor. Soc.,* **61,** 1388–1400.

Douglas, M. W., 1992: Structure and dynamics of two monsoon depressions. Part II: Vorticity and heat budgets. *Mon. Wea. Rev.,* **120,** 1548–1564.

Gill, A. K., 1982: *Atmosphere–Ocean Dynamics.* International Geophysics Series, Vol. 30, Academic Press, 662 pp.

Krishnamurti, T. N., and D. Subrahmanyam, 1982: The 30–50 day mode at 850 mb during MONEX. *J. Atmos. Sci.,* **39,** 2088–2095.

——, M. Kanamitsu, R. Godbole, C. B. Chang, F. Carr, and J. H. Chow, 1976: Study of a monsoon depression. II: Dynamical structure. *J. Meteor. Soc. Japan,* **54,** 208–225.

——, P. Ardanuy, Y. Ramanathan, and R. Pasch, 1981: On the onset vortex of the summer monsoon. *Mon. Wea. Rev.,* **109,** 344–363.

Kuma, K.-I., 1988: The role of the equatorial heat sources in the western Pacific Ocean on the onset of the Asian summer monsoons of 1986. *J. Meteor. Soc. Japan,* **66,** 399–417.

Kummerow, C., W. Barnes, T. Kozu, J. Shiue, and J. Simpson, 1998: The Tropical Rainfall Measuring Mission (TRMM) sensor package. *J. Atmos. Oceanic Technol.,* **15,** 809–816.

——, and Coauthors, 2000: The status of the Tropical Rainfall Measuring Mission (TRMM) after two years in orbit. *J. Appl. Meteor.,* **39,** 1965–1982.

Luo, H., and M. Yanai, 1984: The large-scale circulation and heat sources over the Tibetan Plateau and surrounding areas during the early summer of 1979. Part II: Heat and moisture budgets. *Mon. Wea. Rev.,* **112,** 966–989.

Madden, R. A., and P. R. Julian, 1972: Description of global-scale circulation cells in the Tropics with a 40–50 day period. *J. Atmos. Sci.,* **29,** 1109–1123.

Murakami, T., L. X. Chen, and A. Xie, 1986: Relationship among seasonal cycles, low-frequency oscillations, and transient disturbances as revealed from outgoing longwave radiation data. *Mon. Wea. Rev.,* **114,** 1456–1465.

Potty, K. V. J., U. C. Mohanty, and S. Raman, 2000: Numerical simulation of monsoon depressions over India with a high-resolution nested regional model. *Meteor. Appl.,* **7,** 45–60.

Rao, K. V., and S. Rajamani, 1970: Diagnostic study of a monsoon depression by geostrophic baroclinic model. *Indian J. Meteor. Geophys.,* **21,** 187–194.

Rao, Y. P., 1976: Southwest monsoon. *Synoptic Meteorology, Meteor. Monogr.,* No. 1, India Meteorological Department, 367 pp.

Saha, K., F. Sanders, and J. Shukla, 1981: Westward propagating predecessors of monsoon depressions. *Mon. Wea. Rev.,* **109,** 330–343.

Seko, K., 1987: Seasonal variation of altitudinal dependence of precipitation in Langtang Valley, Nepal Himalaya. *Bull. Glacier Res.,* **5,** 41–47.

Shrestha, M. L., 2000: Interannual variation of summer monsoon rainfall over Nepal and its relation to Southern Oscillation Index. *Meteor. Atmos. Phys.,* **75,** 21–28.

Singh, P., K. S. Ramasastri, and N. Kumar, 1995: Topographical in-

fluence on precipitation distribution in different ranges of Western Himalayas. *Nord. Hydrol.,* **26,** 259–284.

Steiner, M., R. A. Houze Jr., and S. E. Yuter, 1995: Climatological characterization of three-dimensional storm structure from operational radar and rain gauge data. *J. Appl. Meteor.,* **34,** 1978–2007.

Wang, B., and X. Xu, 1997: Northern Hemisphere summer monsoon singularities and climatological seasonal oscillation. *J. Climate,* **10,** 1071–1085.

Wu, M. L. C., S. Schubert, and N. E. Huang, 1999: The development of the South Asian summer monsoon and the Intraseasonal Oscillation. *J. Climate,* **12,** 2054–2075.